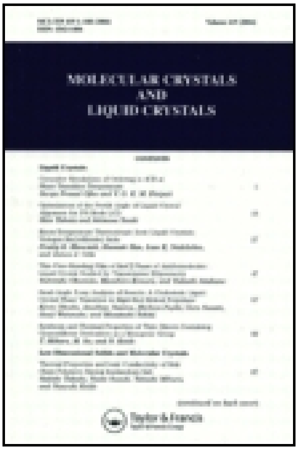

Molecular Crystals and Liquid Crystals
Publication details, including instructions for authors and subscription information:
http://www.tandfonline.com/loi/gmcl20

MOLECULAR DYNAMICS SIMULATIONS OF LIQUID CRYSTAL MOLECULES AT AN AIR-WATER INTERFACE

Makoto Yoneya [a] [b] , Keiko M. Aoki [a] , Yuka Tabe [a] [c] & Hiroshi Yokoyama [a] [c]

[a] Yokoyama Nano-structured Liquid Crystal Project, ERATO, Japan Science and Technology Corporation, 5-9-9 Tokodai, Tsukuba 300-2635, Japan

[b] Hitachi Research Laboratory, Hitachi, Ltd.

[c] Nanotechnology Research Institute, AIST 1-1-4 Umezono, Tsukuba 305-8568, Japan

To cite this article: Makoto Yoneya, Keiko M. Aoki, Yuka Tabe & Hiroshi Yokoyama (2004): MOLECULAR DYNAMICS SIMULATIONS OF LIQUID CRYSTAL MOLECULES AT AN AIR-WATER INTERFACE, Molecular Crystals and Liquid Crystals, 413:1, 161-169

To link to this article: http://dx.doi.org/10.1080/15421400490437196

Mol. Cryst. Liq. Cryst., Vol. 413, pp. 161/[2297]–169/[2305], 2004
Copyright © Taylor & Francis Inc.
ISSN: 1542-1406 print/1563-5287 online
DOI: 10.1080/15421400490437196

MOLECULAR DYNAMICS SIMULATIONS OF LIQUID CRYSTAL MOLECULES AT AN AIR-WATER INTERFACE

Makoto Yoneya and Keiko M. Aoki*
Yokoyama Nano-structured Liquid Crystal Project,
ERATO, Japan Science and Technology Corporation,
5-9-9 Tokodai, Tsukuba 300-2635, Japan

Yuka Tabe and Hiroshi Yokoyama
Yokoyama Nano-structured Liquid Crystal Project,
ERATO, Japan Science and Technology Corporation,
5-9-9 Tokodai, Tsukuba 300-2635, Japan
and
Nanotechnology Research Institute, AIST 1-1-4 Umezono,
Tsukuba 305-8568, Japan

Molecular dynamics simulations were done for terminally alkyl and alkoxy substituted azobenzene liquid crystal (LC) molecules at an air-water interface using realistic (LC and water) molecular models. The simulation result were compared with those of a corresponding amphiphilic modification, i.e. terminal ω-carboxyalkoxy substituted azobenzene. Comparison with a LC with a different mesogen core, phenylpyrimidine, was also made. The interaction energetics were found to be more or less similar both in the alkyl and alkoxy terminated azobenzene and its amphiphilic modification, i.e. cohesive energy dominated over adhesive energy. In contrast, a large difference was found between alkyl and alkoxy terminated azobenzene and phenylpyrimidine LCs; cohesive and adhesive energy contributions were competitive in the latter molecule.

Keywords: amphiphile; Langmuir monolayer; molecular simulation

We would like to thank the members of the Yokoyama Nano-structured Liquid Crystal Project, especially Dr. Takahiro Yamamoto for stimulating discussions.

*also at Hitachi Research Laboratory, Hitachi, Ltd.

Address correspondence to Makoto Yoneya, Yokoyama Nano-Structured Liquid Crystal Project, ERATO, Japan Science and Technology Corporation, 5-9-9 Tokodai, Tsukuba 300-2635, Japan.

INTRODUCTION

It has long been believed that the formation of Langmuir monolayers at an air-water interface is limited to amphiphilic molecules containing a hydrophobic chain and a hydrophilic head group (e.g. -COOH). However, our recent experiments on more than 30 alkyl and/or alkoxy terminated molecules have all shown stable monolayer formations at the air-water interface if they have liquid crystal (LC) phase in bulk [1,2]. Although some dialkyl-terminated thermotropic LC molecules are known to be able to form stable Langmuir monolayers [3], our systematic investigation results led us to believe that monolayer formations with alkyl and/or alkoxy terminated LC molecules are a rather general phenomenon. However, such a non-amphiphilic route to monolayer formation is not understood yet.

In this study, we apply molecular simulations to look at monolayer formation paying special attentions to the LC - water interactions. We also discuss the possibility of a two-dimensional nematic phase with a bolaamphiphilic, a hydrophilic group at both ends, which was suggested by de Gennes [4].

SIMULATION MODEL AND METHOD

Molecular dynamics (MD) simulations were done for systems with the various spreading molecules shown in Figure 1 and a water molecule layer. All these molecules, except 22COOH, have bulk LC phase(s) [5,6]. The SPC (simple point charge) water model [7] was used for the water model in the subphase. The model utilized for spreading molecules was a detailed

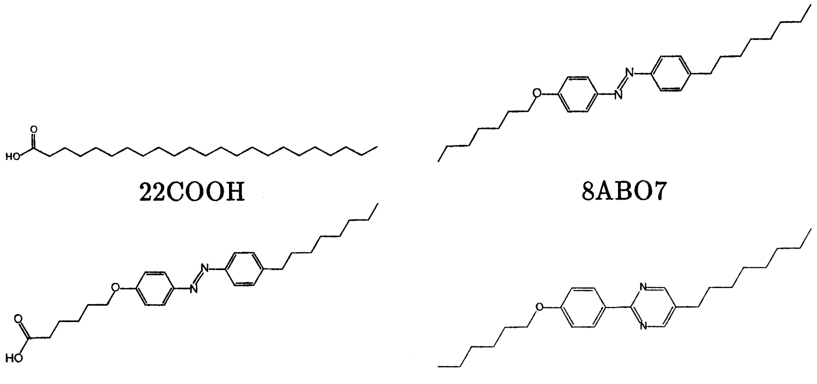

22COOH

8ABO7

8ABO5COOH

8PYPO6

FIGURE 1 Simulated spreading molecules.

atomic model using "united" atoms for all hydrogen atoms (e.g. in the CH_n groups), except for the hydroxyl hydrogen. Hydrogen bond interactions were modeled with simple Coulombic interactions between these hydrogens and corresponding atoms [8]. Atomic charges were obtained from semi-empirical molecular orbital calculations using the program MOPAC-AM1 as the electrostatic potential charge. Each spreading molecule was treated as a flexible model, except that all the bond stretching degrees of freedom were constrained to their equilibrium bond lengths. The inter- and intra-molecular interaction potential function employed was basically the GROMOS-87 potential [8], and we supplied some additional parameters using the results of MOPAC calculations and reference to similar GROMOS parameters.

The simulations were done with a system of various numbers (16–50) of spreading molecules on a pre-equilibrated water layer ($\sim$2 nm thick) composed of 864 (with X-Y dimensions of 3.72×3.72 nm) SPC water molecules, placed in a rectangular MD cell (with the above X-Y dimensions and 20 nm in Z) under periodic boundary conditions. Water molecules in one third (opposite side from the spreading molecules) of the total layer were position restrained (with a force constant of $100\,\mathrm{kJ\,mol^{-1}\,nm^{-2}}$) against the initial equilibrated coordinates in order to keep the layer structure. Charge group-based twin-range 1.0 nm van der Waals and 1.4 nm electrostatic cutoff distances were applied to non-bonded interactions [9]. Trajectories were produced by the MD program package GROMACS (version 3.0) [9] with the leap-frog time integrations and LINCS bond constraint [10] by using a 2fs time step.

After a few thousand steps of the steepest descent energy minimization and initial MD runs, production MD runs up to 21ns were carried out at constant temperature around 300 K under weak couplings to the heat bath (with a time constant of 0.1ps) [11].

RESULTS

Energetics

We first investigated the energetics of the various spreading molecules at the air-water interface and their variation with surface density. The simulations were done starting at a relatively high surface density (e.g. 50 molecules on the 3.72×3.72 nm area water surface) system and then equilibrated MD runs (2–4ns) were done at this density. After the equilibration, a few (2–4) molecules were randomly subtracted from the system while keeping the same water surface area to lower the surface density, then it was allowed to re-equilibrate. The same procedures were repeated to get the surface density dependency of the system energetics.

The calculated surface density ranges were adjusted to the experimentally observed values for the monolayer formations. Representative simulations snapshots from these MD runs are shown in Figure 2.

Equilibrated interaction potential energies per spreading molecules (negative value correspond to structure stabilizing energy) are plotted against area/molecule in Figure 3. This figure shows general trends of increasing cohesive energy and decreasing adhesive energy with decreasing area/molecule (increasing surface density). Within the area/molecule range, we found cohesive *energy* dominated the adhesive *energy* irrespective of whether the spreading molecule had a polar head group (22COOH and 8ABO5COOH) or not (8ABO7). In contrast, cohesive and adhesive energy contributions were competitive in 8PYPO6 (phenylpyrimidine core LC). More precise decompositions to Coulomb and van der Waals contributions for each cohesive and adhesive energy are shown in Figure 4 for 8ABO7, 8ABO5COOH and 8PYPO6 at high surface density. Between 8ABO5COOH and 8ABO7, energetics are similar except the Coulombic-adhesion contribution. Whereas in 8PYPO6, the Coulombic-cohesion contribution is repulsive and this is why 8PYPO6 molecule had a small difference between its cohesive and adhesive contribution. The relatively low total cohesive energy obtained for 8PYPO6 seemed to correspond to our experimental finding that the spreading ability of 8PYPO6 was exceptionally good (it spontaneously spread even from bulk without dissolving in any solvents) compared to common amphiphilic molecules (e.g. stearic acid needs to be dissolved in order to spread).

Structures

In the previous section, we found the overall energetics did not differ much between the non-amphiphilic (alkyl and alkoxy terminated) LC (8ABO7) and its amphiphilic modification (8ABO5COOH). However, for an amphiphilic molecule, the molecular up-down symmetry was clearly broken by the interaction between the hydrophobic head group and water molecules whereas the symmetry could be different in the non-amphiphilic molecule. To clarify this up-down symmetry behavior, we plot the time evolutions of molecular polar tilt angle distribution functions in Figure 5 for the MD simulations of the 8PYPO6 molecule at area/molecule $0.433\,\mathrm{nm}^2$. Here the polar tilt angel was defined as the angle between the interface normal vector and the vector from the end carbon atom of the pyrimidine ring to that of the phenyl ring. The starting configuration was anti-parallel, i.e. the tilt angle distributions were two delta peaks at O° and 180°. After 2ns MD run, the distribution was equilibrated to the two peaks around 60° and 120°. These two peaks were almost comparable in their heights and no clear up-down symmetry breaking was found.

22COOH

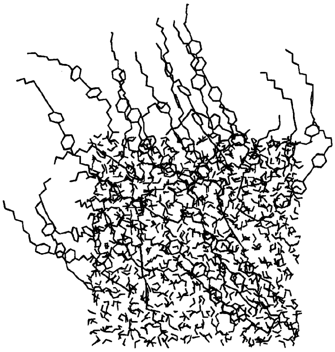

8ABO5COOH

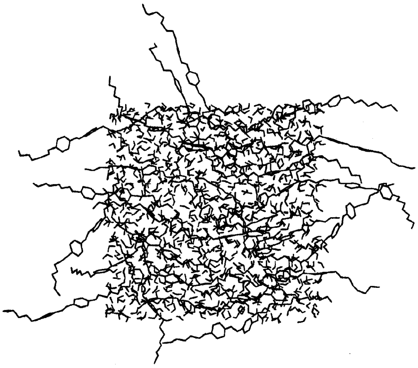

8ABO7

FIGURE 2 Snapshots viewed from the water-layer normal direction (area/ molecule = 0.433 nm^2).

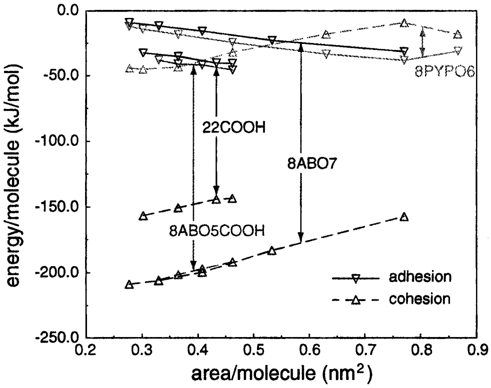

FIGURE 3 Variations of interaction potential energies per spreading molecules against area/molecule. Here, cohesion and adhesion correspond to the interaction energy between spreading molecules and spreading-molecules and water, respectively.

This symmetry difference was also remarkable in the pre-formation stage simulations of the monolayer. In the case of amphiphilic molecules, the structure was more or less like grass growing in a field when a strong wind blows, i.e. the head group was always trapped in the water layer, just like the grass roots were held in the ground. By contrast non-amphiphilic LC molecules were generally lying almost flat at the air-water interface in low surface density regions. In Figure 3, the cohesive and adhesive contributions were crossed around 0.5 nm^2 for 8PYPO6. This crossing area/molecule value roughly corresponded to the remarkable kink (discontinuity)

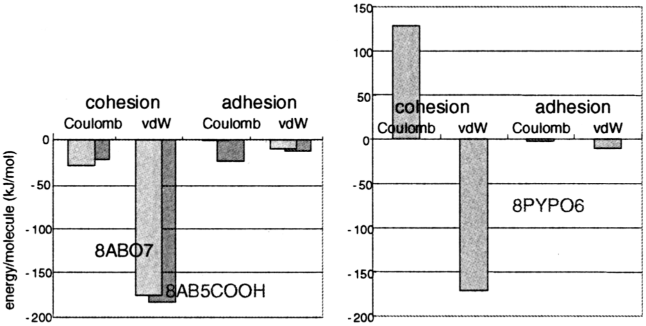

FIGURE 4 Energy decompositions to Coulomb and van der Waals (denoted vdW in the figure) contributions for various spreading molecules at the area/molecule of 0.277 nm^2.

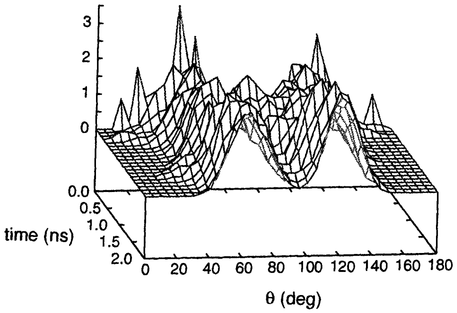

FIGURE 5 Time evolutions of molecular polar tilt angle distribution functions in the 8PYPO6 molecule system.

in the experimental surface pressure vs. area/molecule isotherms. This kink has been considered to be a structural transition of the spreading molecules from flatly lying on the air-water interface to becoming tilted towards it [3]. We then plot the variations of the average tilt of 8PYPO6 molecules against the area/molecule in Figure 6 (the tilt variations for 8ABO7 and 8ABO5COOH are also plotted for comparison). As in the figure, the tilt of 8PYPO6 is increased with area/molecule, but the variations are rather continuous (similar to that of 8ABO7) against the transition model above.

The structures of the subphase were also investigated by plotting polar tilt angle distributions of the water molecules. The distribution functions of the water layers beneath the monolayer with the non-amphiphilic molecule (8ABO7), and its amphiphilic modification (8ABO5COOH), showed no clear difference from the distribution function of the water layer alone.

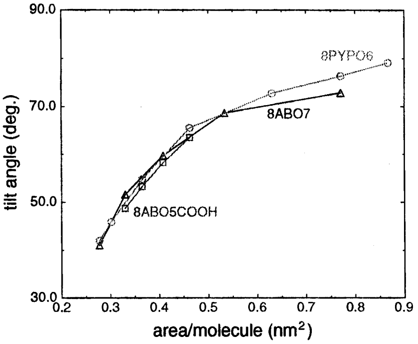

FIGURE 6 Variations of average molecular tilt to the interface (defined as the angle between the interface normal and the vector between each ends of the mesogenic ring system of the molecule).

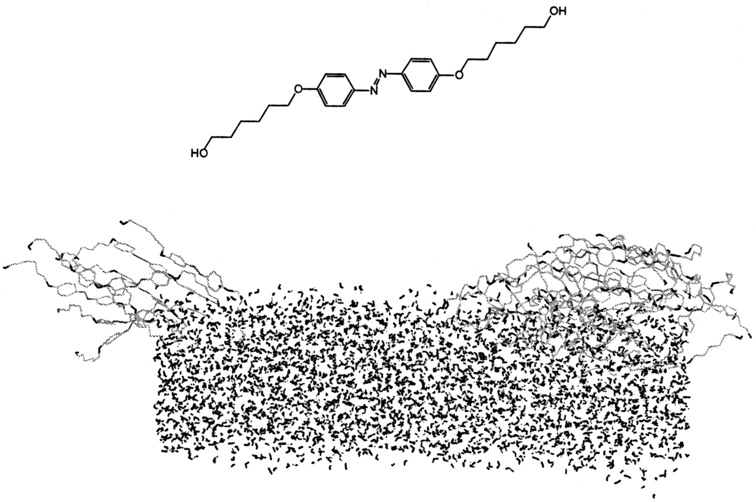

FIGURE 7 Bolaamphiphilic azobenzene and snapshot at area/molecule 1.734 nm^2.

DISCUSSION

As noted in the previous section, non-amphiphilic LC molecules were generally flatly lying on the air-water interface in low surface density regions. Over 30 years ago, de Gennes [4] suggested the possibility of a 2-D nematic phase with bolaamphiphilic LCs (a hydrophilic group at both ends). We have done simulations with the bolaamphiphilic modification of azobenzene shown in Figure 7 (this molecule also has bulk LC phase [12]). A snapshot of MD with the bolaamphiphilic azobenzene at low surface density is also reproduced in the figure. This bolaamphiphilic LC molecules were not flatly lying like uniform two-dimensional (2-D) nematic LCs, but aggregated in small clusters (as in 8ABO7) with dominant cohesive interactions. The results suggested that precise molecular design in both molecule symmetry and energetics is necessary to realize the 2-D nematic phase at the air-water interface.

REFERENCES

[1] Tabe, Y., Nishiyama, I., & Yokoyama, H. (2000). In: *Proc. 7th. Int. Display Work-Shops*, Kobe: Japan, 1143.

[2] Tabe, Y., Nishiyama, I., Aoki, K. M., Yoneya, M., & Yokoyama, H. (2000). In: *The 2nd Anglo-Japanese Seminar on Liquid Crystals*, York: UK.

[3] Dörfer, H.-D., Kerscher, W., & Sackmann, H. (1972). *Z. phys. Chemie, Leipzig*, *251*, 314.

[4] de Gennes, P. G. (1971). *Symp. Faraday Soc.*, *5*, 16.

[5] de Jeu, W. H. (1977). *J. Phys.*, *38*, 1265.
[6] Zaschke, V. H. (1975). *J. f. prakt. Chemie*, *317*, 617.
[7] Berendsen, H. J. C., Postma, J. P. M., van Gunsteren, W. F., & Hermans, J. (1981). In: *Intermolecular Forces*, Pullman, B. (Ed.), Reidel: Dordrecht, 331.
[8] van Gunsteren W. F. & Berendsen, H. J. C. (1987). *GROMOS Manual*, BIOMOS b.v., Biomolecular Software, Univ. of Groningen: The Netherlands.
[9] Lindahl, E., Hess, B., & van der Spoel, D. (2001). *J. Molecular Modeling*, *7*, 306.
[10] Hess, B., Bekker, H., Berendsen, H. J. C., & Fraaije, J. G. E. M. (1997). *J. Comput. Chem.*, *18*, 1463.
[11] Berendsen, H. J. C., Postma, J. P. M., van Gunsteren, W. F., DiNola, A., & Haak, J. R. (1984). *J. Chem. Phys.*, *81*, 3684.
[12] Kapitza, H. & Zentel, R. (1988). *Macromol. Chem.*, *189*, 1793.